LBL-37280
UC-413
Preprint

Lawrence Berkeley Laboratory
UNIVERSITY OF CALIFORNIA

Submitted to Journal of Applied Physics

Low-Background Instrumental Neutron Activation Analysis of Silicon Semiconductor Materials

A.R. Smith, R.J. McDonald, H. Manini, D.L. Hurley,
E.B. Norman, M.C. Vella, and R.W. Odom

May 1995

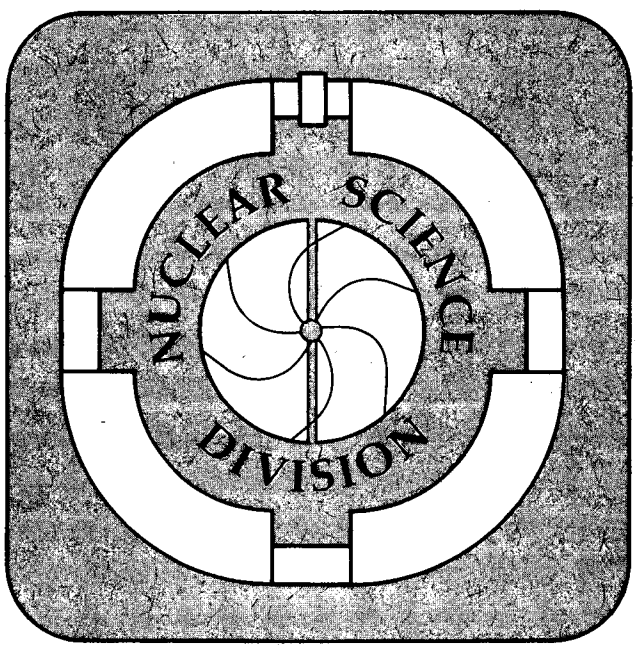

REFERENCE COPY
Does Not
Circulate
LBL-37280
Copy 1
Bldg. 50 Library.

Prepared for the U.S. Department of Energy under Contract Number DE-AC03-76SF0009

DISCLAIMER

This document was prepared as an account of work sponsored by the United States Government. While this document is believed to contain correct information, neither the United States Government nor any agency thereof, nor The Regents of the University of California, nor any of their employees, makes any warranty, express or implied, or assumes any legal responsibility for the accuracy, completeness, or usefulness of any information, apparatus, product, or process disclosed, or represents that its use would not infringe privately owned rights. Reference herein to any specific commercial product, process, or service by its trade name, trademark, manufacturer, or otherwise, does not necessarily constitute or imply its endorsement, recommendation, or favoring by the United States Government or any agency thereof, or The Regents of the University of California. The views and opinions of authors expressed herein do not necessarily state or reflect those of the United States Government or any agency thereof, or The Regents of the University of California.

This report has been reproduced directly from the best available copy

Lawrence Berkeley Laboratory is an equal opportunity employer.

DISCLAIMER

This document was prepared as an account of work sponsored by the United States Government. While this document is believed to contain correct information, neither the United States Government nor any agency thereof, nor the Regents of the University of California, nor any of their employees, makes any warranty, express or implied, or assumes any legal responsibility for the accuracy, completeness, or usefulness of any information, apparatus, product, or process disclosed, or represents that its use would not infringe privately owned rights. Reference herein to any specific commercial product, process, or service by its trade name, trademark, manufacturer, or otherwise, does not necessarily constitute or imply its endorsement, recommendation, or favoring by the United States Government or any agency thereof, or the Regents of the University of California. The views and opinions of authors expressed herein do not necessarily state or reflect those of the United States Government or any agency thereof or the Regents of the University of California.

LBL-37280
UC-413

Low-Background Instrumental Neutron Activation Analysis of Silicon Semiconductor Materials

A.R. Smith, R.J. McDonald, H. Manini, D.L. Hurley, and E.B. Norman

Nuclear Science Division
Lawrence Berkeley Laboratory
University of California
Berkeley, California 94720

M.C. Vella

Accelerator and Fusion Research Division
Lawrence Berkeley Laboratory
University of California
Berkeley, California 94720

R.W. Odom

Charles Evans and Associates
Redwood City, California 94063

May 1995

This work was supported in part by the Director, Office of Energy Research, Office of High Energy and Nuclear Physics, Division of High Energy Physics, of the U.S. Department of Energy under Contract No. DE-AC03-76SF00098.

Low-Background Instrumental Neutron Activation Analysis of Silicon Semiconductor Materials

A.R. Smith, R.J. McDonald, H. Manini, D.L. Hurley, and E.B. Norman

Nuclear Science Division

M.C. Vella

Accelerator & Fusion Research Division

Lawrence Berkeley Laboratory
Berkeley, CA 94720

R.W. Odom

Charles Evans & Associates
Redwood City, CA 94063

ABSTRACT

Samples of silicon wafers, some implanted with zinc, some with memory circuits fabricated on them, and some with oxide coatings were activated with neutrons and analyzed for trace element impurities with low-background germanium gamma-ray spectrometers. Results are presented for these samples as well as for a reference material. Because the silicon matrix activation is so small, reduced spectrometer system background permits the detection of significantly lower impurity concentrations than would otherwise be possible. For our highest efficiency and lowest background system, limits on the lowest levels of trace element concentrations have been measured for wafer sized (1-10 gram) samples and inferred for bulk sized (360 gram) samples. For wafer-sized samples, parts-per-trillion detection capabilities are demonstrated for a variety of elemental contaminants important in semiconductor fabrication.

1. Introduction

Instrumental Neutron Activation Analysis (INAA) has become a common method of trace element analysis since the advent of efficient high-resolution germanium (Ge) gamma-ray spectrometers in the 1970s. These spectrometers allow the quantification of a large number of gamma-ray-emitting nuclei based on the energy and intensity of their characteristic gamma rays. Since the sensitivity to trace elements in a host material is dependent on the extent of neutron activation of the host, the ultra-pure silicon used in semiconductor fabrication is an ideal matrix for trace element analysis via INAA. Even after prolonged exposure within a nuclear reactor, minimal observable gamma-ray-emitting activities are produced in the silicon. Studies described in the literature, for example References 1-3, show that INAA can provide high sensitivity to selected contaminants in silicon. This work describes the ultra high sensitivity that can be achieved by using a high-efficiency spectrometer in a very low-background counting facility.

Because the silicon matrix activation is minimal, ultimate detection sensitivity depends critically on reducing the external background seen by the spectrometers. The Lawrence Berkeley Laboratory (LBL) has such dedicated Low Background Facilities (LBF) with sites at Berkeley and Oroville. Spectrometers at the Berkeley site are housed in 10 cm thick low-activity lead isolation shields that are located in a room-sized laboratory surrounded by 1.5 meters of low-activity concrete. At the Oroville site, the low-activity detector system is housed in a 15-20 cm thick low-activity lead shield, which in turn is located in the power house of the Oroville Dam (a California Department of Water Resources Facility) under a 180 meter thick layer of bedrock and fill. At both sites, the shielding effectively eliminates interference from external terrestrial gamma-ray emitters. At the Berkeley site, the detector background (BKG) response is dominated by the effects of cosmic ray interactions in the neighborhood of the detector. At the Oroville site, where the cosmic ray intensity has been reduced 1000-fold with respect to the surface intensity, the detector BKG response is dominated by the very small residual activity in the detector assembly itself. Sensitivity at the Oroville site is about 10 times higher than that at the Berkeley site.

It is instructive to see the advantage INAA has for high-purity silicon compared to earth-like materials with typical concentrations of many trace elements. An example material is the "standard pottery" (Reference 4) prepared at LBL and used for decades as a comparison standard for studies of ancient pottery and other earth materials. The upper curve of Figure 1 shows a spectrum taken from a 0.020 gram sample of the standard pottery irradiated with 9.6E16 ($=9.6 \times 10^{16}$) neutrons/cm^2 and counted 8 days after irradiation. At this time, the Compton-scattered continuum of gamma rays from the 889 and 1120 keV characteristic ^{46}Sc decay lines (and their 2010 keV sum line) dominate the spectrum. The Compton distribution as measured below the 889 and 1120 keV gamma rays is 600 to 800 times greater than system background. The summed distribution between 1120 and the 2010 keV (sum) peak ranges from 200 to 400 times system background. In sharp contrast to this is the spectrum from a sample of float-zone silicon (normalized to correspond to equal neutron fluence, mass, and counting time) shown in the lower part of Figure 1. This spectrum shows a few small peaks, some from natural background and some from minute activation products in the silicon, superimposed on a continuum that is essentially system background. Although each peak contributes Compton-scattered gamma rays to the continuum, this contribution is typically 1-2% in height compared to the height of the peak itself. Thus, the system background is the only interfering activity, and may be used to calculate the Interference-Free Detection Limits (IFDL) referred to in Reference 3 and shown, for this work, in Table VIII. Under these circumstances, a low-background facility is key to achieving low detection limits to impurities in silicon via INAA.

This paper describes a program to demonstrate the sensitivity of the LBF for detecting selected contaminants in silicon (Si) and silicon dioxide (SiO_2) using INAA. Results are presented for Si and SiO_2, zinc implanted Si, memory circuit fabrications, and "standard pottery" reference samples prepared at LBL.

2. Procedures

Samples were prepared from pieces of Si wafers or from whole 100 mm diameter Si wafers, about 0.5 mm thick. When necessary, these pieces were scored and broken under clean-room conditions to fit into 1.7 cm diameter by 10 cm long quartz tubes. The tubes were evacuated, sealed, and sent to the University of Missouri Research Reactor for irradiation. All irradiations were done utilizing a flux of 8.0E13 neutrons/cm^2/sec. Activation times of 20 minutes to 10 hours were used. The samples were shipped to the LBF via overnight air freight. The quartz tubes were broken open and the samples cleaned with distilled water and placed in plastic boxes prior to counting.

The initial counting took place on a 30% (relative to a 7.6 cm x 7.6 cm NaI) p-type Ge spectrometer with an active cosmic-ray shield at the LBF Berkeley site. Detector resolution at 1333 keV was measured to be 1.85 keV. Subsequent counting took place on a 115% n-type Ge spectrometer at the Oroville site. This spectrometer provided 2.3 keV resolution at 1333 keV. Data acquisition was performed with the ORTEC MAESTRO II program running on a PC, and counting times varied from a few hours to a week. 8192 channel spectra were taken over a range from 40-3500 keV.

Detector efficiency as a function of gamma ray energy was determined from radioactive sources. The primary source used was a sample of pulverized uranium ore in fine-ground serpentine containing 4.04 ±0.0016 per cent U by weight and in secular equilibrium with daughter products as certified by the New Brunswick Laboratory. This material was mixed with epoxy to form a 5 cm diameter by 0.2 cm thick disk containing a total of 0.0404 grams of uranium which produces 500 decays/sec. Decay rates for individual gamma-rays were calculated from the decay rate and the intensities (in gamma-rays per 100 decays) listed in Reference 5. Efficiency versus energy curves were established by comparing these emission rates with detection rates.

Unsummed transitions formed the basic efficiency function while summed transitions (where cascade transitions are summed in the detector) allowed us to determine summing corrections (15-27% for a two-gamma-ray cascade). Efficiency values for energies below 200 keV were read off the graph; those above 200 keV were calculated from a power-law function. Efficiency corrections due to source size were calculated using the algorithms developed in Chapter 4 of Reference 6. These corrections were <20%. For cases where counting statistics are not the limiting factor, uncertainty in geometrical and summing corrections account for the major component of the overall uncertainty in concentrations.

Each run was analyzed with the program SAMPO (Reference 7) and gamma-ray peak areas were determined for all statistically significant gamma rays. Constants corresponding to counting time, decay time, sample mass and peak areas were entered into the PANORAMA spreadsheet on the MACINTOSH. Nuclear decay parameters were obtained from References 8-9 and cross-sections were obtained from Reference 10. The details of these calculations, including decay-time corrections, are discussed in the Appendix. The measured and actual energy of the gamma rays needed to agree to within ±0.3 keV to be assigned to a particular decay. Following data entry, the spreadsheet is sorted by mass and the data is checked to see that no weaker lines are accepted in the absence of stronger lines. Unobserved gamma rays are removed from the spreadsheet and a macro calculation is performed. The macro-calculated concentrations and other selected information are then printed out. When possible, several characteristic transitions from a nuclear decay were used to determine activity.

This is essentially a "first principles" method, relying on explicit knowledge of reactor parameters, nuclear data, and detector response. The manifold uncertainties associated with this technique limits its accuracy, but allows one to search for essentially all the elements in the periodic table accessible to INAA.

Verification of this method comes from analysis of the "standard pottery" discussed in the introduction. Samples of about 0.020g (weighed to 1%) were encapsulated in aluminum discs of 99.9999% purity and sent to the reactor. "Blank" disc capsules were also sent so we could subtract the activation products from the Al to determine the concentrations in the pottery alone. As shown in Table I, our concentrations, determined by the procedure described above, agree well with the accepted concentrations in the standard pottery for 22 of the 24 elements listed. Only As and Ba give results that disagree.

For the best precision, particularly where one is looking for a limited number of contaminants, one may use a system of "monitors" or "standard materials", irradiated under identical conditions and then compared to the "unknowns" in the sample. This method eliminates most of the uncertainties described above, and ultimately can provide precision measurements, approaching 1% uncertainty for favorable cases.

3. Results

3.1 Float-Zone Silicon:

The purpose of this study was to demonstrate LBF detection limits with a clean Si substrate. Because INAA is a volume process, it is as sensitive to surface contamination as it is to bulk contamination. This sample was irradiated for ten hours, separated into two parts, and counted at the LBF Berkeley site to determine total trace element concentrations. The trace-element profiles for the two parts were nearly identical. We then performed a heavy etch, utilizing a solution of concentrated nitric and hydrofluoric acids, until about 10% of the material was removed. This enabled us to separate surface contamination from bulk impurities. Figure 2 shows the spectrum before and after etching. Since so little activity remained after etching, the samples were combined and counted at the LBF Oroville site. Table II shows data for 15 elements observed. Column 2 shows concentrations from sample #1 before etching and Column 3 shows concentrations from the same sample following etching. These samples were both counted at the Berkeley site. Columns

4 and 5 show results for combined samples of etched Si counted at our higher sensitivity Oroville site at different times after irradiation. Clearly, most of the trace elements observed were on or near the surface. Only small amounts of Cr, As, Sb, and Au are actually in the bulk Si.

3.2 Si and SiO_2 samples:

Samples of Si and SiO_2 were studied to examine the two materials for differences in trace-element concentrations. These samples, prior to irradiation, were treated identically except for the oxidation process. Both samples were cleaned via identical processes, including a "piranha" clean ($H_2SO_4 + H_2O$ at 120°C) to oxidize organics and metals, followed by a 5:1 HF etch to remove the oxide. One sample was then used to grow a 500 nm thick oxide layer in 1.5 hours at 1000°C. Both samples were then subjected to another "piranha" clean followed by cleaning in 1% HF. The samples were then cleaved to fit the quartz vials needed for irradiation in the reactor. All this occurred in a class 100 clean room. The samples were sent to the reactor and exposed for ten hours and returned to the LBF for counting. As shown in Table III, the concentrations of contaminants vary from 0.2 to 2.6 times greater in the oxide material than in the elemental Si, with the average ratio of 1.5.

3.3 ^{64}Zn ion-implanted Si:

Samples of ^{64}Zn ion-implanted Si were obtained from Charles Evans & Associates. These samples were implanted with ^{64}Zn to a nominal density of 1.0E14 atoms/cm^2 and used to test our ability to determine "known" concentrations of contaminants in a sample. The samples, consisting of a number of cm^2-sized wafer pieces, were irradiated for one hour and returned to the LBF for counting. They were arranged on the detector surface to approximate the same geometry as our U calibration source. Results from the Berkeley site and the higher sensitivity Oroville site are in near-perfect agreement. As shown in the top rows of Table IV, the observed concentration of 6.15±0.4 E13 is substantially lower than the 1.0E14 atoms/cm^2 expected.

In order to test whether this could be due to large non uniformities in the sample, the six largest pieces were counted separately. Since these samples were each smaller than the calibration sample, a geometrical correction of 18% (calculated according to the algorithms in chapter 4 of Reference 6) was made to the detector efficiency value. The lower part of Table IV shows these results, where the quoted uncertainties are due only to counting statistics. While the spread in this data exceeds the statistical uncertainty, it is still only ±5% and thus is consistent with only small variations in uniformity. We conclude that these implants really are about 40% lower in ^{64}Zn concentration than labeled.

In order to learn more about processed Si wafers, we analyzed the data for elements besides Zn. Table V shows these results for two runs: one taken 8.3 days following irradiation and another taken 23 days after irradiation. Concentrations of impurities in an unetched float-zone Si sample are included for perspective. What stands out in this comparison besides the factor of two or so higher concentrations of some elements, is a significant difference in abundance for the Sb isotopes. Concentrations of ^{121}Sb are observed ten times higher than expected for normal isotopic abundance. Analysis from the weak 692.9 keV line as well as the stronger 564.4 keV line confirms this. We speculate that the cause of this may be ^{121}Sb contamination during the implantation process. This is an example of the power of INAA to detect contamination or abnormalities in the processing or handling of Si wafers.

3.4 Memory Circuit Fabrications:

A sample of Si with memory fabricated into it was irradiated for one hour. The goal of this experiment was to see what we could measure of the elements added in processing. Most noticeable in Table VI is the amount of As— 0.8 parts-per-million added as a dopent in the fabrication process! The Fe and Cr observed at similar levels here and in the Zn implant discussed

above may come from stainless steel in the implant tool. Ag and Zn may be due to "flash" layers for metal contact bonding. Clearly, additional studies would be needed to isolate the source of these elements.

3.5 Detection Limits:

The most important aspect of this work was to determine detection limits for as many elements as possible. To do this, background count integrals were measured at or in the vicinity of expected peaks in spectra collected at various times after irradiation (3 days, 9 days, and 58 days). The widths of background regions used were approximately equal to the expected full width at one-tenth-maximum for the peak. Twice the square root of these numbers were plotted on a graph and smoothed. These 2σ limits were input to the spreadsheet as areas and concentrations were calculated. The results are depicted graphically in Figure 3 and listed in Table VII where they are compared to the measurements of Reference 1 which studied samples of similar size. Note that this procedure does not necessarily give optimal limits for each of these isotopes, however, these limits are based on real data with realistic interferences.

The determination of a detection limit for a given element depends critically on interfering activities in the spectra. In the case of short lived elements, e.g. ^{75}As and ^{82}Br, interference from the Compton distribution from the 1368 and 2753 keV gamma rays from the ^{24}Na decay (produced by the ^{28}Si(n,αp)^{24}Na reaction) limits the ultimate sensitivity. Even minute amounts of Au in the sample produce large interferences below 400 keV from ^{198}Au with a half-life of 2.6 days. Thus, determination of detection limits for each element must depend on the other elements present.

These limits are all lower for longer irradiation times and larger samples, particularly for the cases of half-lives longer than a week or so, where the effects of background from ^{24}Na and ^{198}Au are reduced or eliminated. However, extrapolation to larger sample size is not linear for two main

reasons: 1) Size limitations within the reactor require that most larger samples be farther from the core center and see smaller fluxes. 2) Geometric modifications to the detector efficiency and internal absorption, particularly for low-energy gamma rays, means that overall detection efficiency decreases as sample size increases. To estimate these effects, a reasonable "large" sample was considered to be a 10 cm diameter by 2 cm thick disk of volume 157 cm^3 corresponding to 365 grams for silicon. Such a sample would be irradiated in a part of the reactor where the flux was lower. A sample of this size could see a flux of 6.43E12 neutrons/cm^2/second. This would require 124 hours to achieve the same flux integral as our smaller samples and improve sensitivity by greater than a factor of 20.

A 157 cm^3 sample, containing earth materials with known amounts of uranium, was counted to determine the geometrical effect on detector efficiency. For this sample, the count rate increases by a factor of 134 compared to a 1 gram sample, given the elements in equal concentrations. This factor, combined with the assumption that an observable peak is 2 standard deviations above background, generates the list of selected detection limits in Table VIII for the optimal case of Interference Free Detection.

4. Conclusions

This paper describes the beginning of a program at the Low Background Facilities of Lawrence Berkeley Laboratory to apply Instrumental Neutron Activation Analysis to the problem of determining contaminants in silicon semiconductor materials. A variety of samples were investigated, including unprocessed float-zone silicon, silicon wafer material implanted with Zn, memory circuit fabrications, and silicon with a 500 nm oxide layer. Processes, techniques, and databases were developed to carry out this project, and parts-per-trillion sensitivities were obtained for 29 elements in wafer-sized samples. A "standard pottery" material was irradiated and analyzed to verify reactor parameters and calculations.

For samples of pure Si, the interference one works against is essentially system background (for elements with half-lives greater than about one week). The ultimate detection sensitivity for elements in this category depends critically on a low-background counting facility. Detection limits estimated for 0.356 kg-sized samples are at least 20 times lower, assuming similar interference. Interference Free Detection Limits are even lower.

5. Acknowledgments

We thank Jack Walton for providing the comparison samples of Si and SiO_2 and Robert O'Donnell for preparing them. We also thank Frank Asaro for providing the samples of "standard pottery" and aluminum blanks, as well as valuable guidance drawn from his extensive experience in this field.

This work was supported by the Director, Office of Energy Research, Office of High Energy and Nuclear Physics, Division of Nuclear Physics, U.S. Department of Energy under contract No. DE-AC03-76SF00098.

TABLE I

Trace-element Concentrations in PPM in the LBL Standard Pottery

Element	Published Concentration (Ref. 4)	Measured Concentration
Na (^{24}Na)	2610±40	2530±330
K (^{42}K)	13500±400	ND
Sc (^{46}Sc)	20.55±0.33	19.5±1.5
Cr (^{51}Cr)	102±4	102±6
Fe (^{59}Fe)	10170±120	10430±900
Co (^{60}Co)	14.06±0.15	15±1
Zn (^{65}Zn)	68±8	67±6
As (^{76}As)	30.8±2.2	25.5±2.2
Br (^{82}Br)	2.3±0.9	2.24±0.45
Mo (^{99}Mo)	ND	9.8±1.3
Sb (^{122}Sb)	1.66±0.12	2.1±0.3
Sb (^{124}Sb)	1.73±0.06	1.90±0.15
Ba (^{131}Ba)	712±32	500±80
Cs (^{134}Cs)	8.31±0.55	8.25±0.7
La (^{140}La)	44.9±0.45	43.5±3.0
Ce (141Ce)	80.3±3.9	70±9
Nd (^{147}Nd)	ND	35±4
Eu (^{152}Eu)	1.286±0.048	1.2±0.1
Tb (^{160}Tb)	ND	0.80±0.08
Hf (^{181}Hf)	6.23±0.44	6.0±0.8
Ta (^{182}Ta)	1.55±0.044	1.5±0.17
W (^{187}W)	ND	10.3±2
Au (^{198}Au)	<0.01	0.002±0.005
Th (^{233}Pa)	13.96±0.40	15.4±1.4
U (^{239}Np)	4.82±0.44	5.6±0.6

Table I: Concentrations in parts-per-million (PPM) in the standard pottery and 1σ uncertainties. Middle column: Values from Reference 4. Last column: concentrations (in parts-per-million) of elements measured in this study. ND indicates that no activity was observed for this element.

TABLE II

Trace-element Concentration in PPT for Float-zone Silicon Before and After Surface Etching

Element	Si #1 T_D=3.2 Day Unetched Concentration	Si #1 T_D=7.1 Day Etched Concentration [2]	Si (6.9g) T_D=9.0 Day Etched Concentration	Si (6.9g) T_D=58 Day Etched Concentration
Na (^{24}Na) [1]	4700±250	240±20	300±24	ND
K (^{42}K)	154±11	ND	ND	ND
Sc (^{46}Sc)	0.49±0.09	ND	ND	ND
Cr (^{51}Cr)	185±13	ND	0.95±0.1	1.0±0.2
Fe (^{59}Fe)	5900±900	ND	ND	ND
Zn (^{65}Zn)	2360±140	ND	ND	ND
As (^{76}As)	12.2±0.9	11.0±0.7	10.5±0.8	ND
Br (^{82}Br)	370±40	ND	ND	ND
Mo (^{99}Mo)	68±9	ND	ND	ND
Ag (^{110m}Ag)	370±40	ND	ND	ND
Sb (^{124}Sb)	39±3	0.39±0.05	0.39±0.04	0.43±0.03
La (^{140}La)	5.3±0.3	ND	ND	ND
Ce (^{141}Ce)	34±6	ND	ND	ND
W (^{187}W)	4.8±0.5	ND	ND	ND
Au (^{198}Au)	170±6	2.7±0.3	8.0±0.3	ND

Table II: 15 element table of contamination in parts-per-trillion (PPT) observed before (column 2) and after (columns 3 - 5) etching. ND indicates that no activity was observed. T_D is the time between the end of irradiation and the beginning of counting. Uncertainties are $\pm 1\sigma$.

[1] about 300 PPT equivalent comes from the $^{28}Si(n,\alpha p)^{24}Na$ reaction from high energy neutrons.

[2] This was a short run compared to the others.

TABLE III

Trace-element Concentrations in PPT for samples of Si and SiO_2

Element	Concentrations in Silicon	Concentrations in Silicon Dioxide	Concentration Ratio: SiO_2 /Si
Na (^{24}Na) [1]	5000±270	7830±510	1.6
Sc (^{46}Sc)	0.39±0.04	0.81±0.05	2.1
Cr (^{51}Cr)	2110±80	2600±100	1.2
Fe (^{59}Fe)	26900±1900	33700±2500	1.3
Co (^{60}Co)	24.0±1.7	43.3±2.5	1.8
Zn (^{65}Zn)	1920±104	3790±190	2.0
As (^{76}As)	11.1±0.9	14.3±1.4	1.3
Br (^{82}Br)	2.7±0.6	6.7±1	2.5
Zr (^{95}Zr)	780±130	2000±200	2.6
Mo (^{99}Mo)	97±12	245±30	2.5
Ag (^{110m}Ag)	34±4	60±6	1.8
Sb (^{122}Sb)	20.2±1.4	26.9±1.9	1.3
Sb (^{124}Sb)	14.6±1.2	19.8±1.6	1.4
La (^{140}La)	190±11	36.3±2	0.20
Ce (^{141}Ce)	780±97	1040±130	1.3
Nd (^{147}Nd)	146±25	ND	ND
W (^{187}W)	62±4	100±7	1.6
Au (^{198}Au)	77±3	57±2	0.74
Hg (^{203}Hg)	129±5	65±3	0.50
U (^{239}Np)	<11	9.0±1	>0.82

Table III: 20 element table of trace elements concentrations in parts-per-trillion (PPT) observed in identically-handled samples of Si and SiO_2. Uncertainties are $\pm 1\sigma$. ND indicates that no activity was observed. Both samples were counted at about 6 days after irradiation.

[1] about 300 PPT equivalent comes from the $^{28}Si(n,\alpha p)^{24}Na$ reaction from high energy neutrons.

TABLE IV

Concentration of ^{64}Zn in the Implant

Run Number	Site	T_D	mass	Concentration (x 10^{13} Atoms/cm^2)
1	Berkeley	8 day	1.1g	6.17±0.4
2	Oroville	23 day	1.1	6.13±0.4
			Average	6.15±0.3
3	Oroville	30 day	0.179	6.33±0.12
4	Oroville	31 day	0.115	5.85±0.16
5	Oroville	32 day	0.118	5.78±0.15
6	Oroville	33 day	0.102	6.04±0.20
7	Oroville	34 day	0.088	6.32±0.19
8	Oroville	36 day	0.094	6.44±0.21
			Average	6.13±0.08

Table IV: Top two rows: Determination of ^{64}Zn surface concentrations based on counts of the total sample. $\pm 1\sigma$ uncertainties include counting statistics and systematic uncertainties. Next 6 rows: Determination of ^{64}Zn surface concentrations for individual pieces to show uniformity. Only the $\pm 1\sigma$ counting statistics are included in the uncertainties. T_D is the time between the end of irradiation and the beginning of counting.

TABLE V

Trace-Element Concentration in PPT in ^{64}Zn Implant

Element	Run 2 T_D=23 Day Concentrations	Run 1 T_D=8.3 Day Concentrations	Si (3.005g) T_D=3.2 Day Concentrations
Na (^{24}Na) [1]	ND	ND	4700±250
K(^{42}K)	ND	ND	154±11
Sc (^{46}Sc)	ND	ND	0.49±0.09
Cr (^{51}Cr)	1330±70	1520±94	185±13
Fe (^{59}Fe)	12200±1000	15000±3000	5900±900
Co (^{60}Co)	37.5±3	ND	ND
Br (^{82}Br)	ND	1400±180	ND
As (^{75}As)	ND	ND	12.2±0.9
Mo (^{99}Mo)	ND	ND	68±9
Ag (^{110m}Ag)	66±9	108±20	370±40
Sb (^{122}Sb)	ND	480±39	48±3
Sb (^{124}Sb)	31±3	32.4±4.5	39±3
Ba (^{131}Ba)	4000±700	4500±800	ND
La (^{140}La)	ND	11.5±2	5.3±0.3
Ce (^{141}Ce)	30±6	ND	34±6
Eu (^{152}Eu)	1.7±0.4	ND	ND
Hf (^{181}Hf)	14.5±2	ND	ND
Ta (^{182}Ta)	31±3	30±5	ND
W(^{187}W)	ND	ND	4.8±0.5
Au (^{198}Au)	99±5	105±5	170±6

Table V: Other elements and their concentrations in parts-per-trillion (PPT) observed in the Zn implant samples with $\pm 1\sigma$ uncertainties. Run 2 was counted at the Oroville site and run 1 was counted at the lower-sensitivity Berkeley site. The column labeled Si(3.005g) refers to the first count of the unetched float zone Si and is included for comparison. ND indicates that no activity was observed.

[1] about 300 PPT equivalent comes from the $^{28}Si(n,\alpha p)^{24}Na$ reaction from high energy neutrons.

TABLE VI

Trace-element Concentrations in PPT in the Memory Fabrications

Element	Concentration
Na (^{24}Na) [1]	24600±4000
Sc (^{46}Sc)	1.1±0.1
Cr (^{51}Cr)	450±30
Fe (^{59}Fe)	12000±1500
Co (^{60}Co)	37±4
Zn (^{65}Zn)	8500±550
As (^{76}As)	800,000±70,000
Ag (^{110m}Ag)	1670±170
Sb (^{124}Sb)	105±9
Au (^{197}Au)	370±20

Table VI: 10 element table of trace elements concentrations in parts-per-trillion (PPT) observed in the memory fabrications. Uncertainties are $\pm 1\sigma$.

[1] about 300 PPT equivalent comes from the ^{28}Si(n,αp)^{24}Na reaction from high energy neutrons.

TABLE VII

Wafer-sized Sample Detection Limits (D.L.) in PPT

Element	D.L. This Work	D. L (Ref. 1)	Element	D.L. This Work	D.L. (Ref. 1)
Na (^{24}Na) [1]	<300	500	Ba (^{131}Ba)	5.2	60
K (^{42}K)	140	150	La (^{140}La)	0.018	0.15
Ca(^{47}Ca)	260	10000	Ce (^{141}Ce)	0.43	0.9
Sc(^{46}Sc)	0.0011	0.03	Pr (^{142}Pr)	3.5	6
Cr (^{51}Cr)	0.43	2.	Nd (^{147}Nd)	0.82	10
Fe (^{59}Fe)	8.3	300	Eu (^{152}Eu)	0.0057	0.07
Co (^{60}Co)	0.012	0.5	Gd (^{159}Gd)	0.70	6
Zn (^{65}Zn)	0.35	15	Tb (^{160}Tb)	0.0090	0.1
As (^{76}As)	0.16	NL[2]	Ho (^{166}Ho)	1.2	3
Se (^{75}Se)	0.27	2	Yb (^{175}Yb)	0.045	0.2
Br (^{82}Br)	0.25	NL[2]	Lu (^{177}Lu)	0.011	0.04
Sr (^{85}Sr)	7.9	150	Hf (^{181}Hf)	0.026	0.3
Rb (^{86}Rb)	0.34	10	Ta (^{182}Ta)	0.012	0.5
Zr (^{95}Zr)	6.5	150	W (^{187}W)	1.1	NL[2]
Mo (^{99}Mo)	2.0	6	Re (^{186}Re)	0.029	0.3
Ru (^{103}Ru)	0.11	1.5	Os (^{191}Os)	0.14	0.7
Ag (^{110m}Ag)	0.074	3	Ir (^{192}Ir)	0.0010	0.004
Cd (^{115}Cd)	1.5	15	Pt (^{195m}Pt)	22	4
Sn (^{113}Sn)	9.5	200	Au (^{198}Au)	0.0010	NL [2]
Sb (^{122}Sb)	0.017	NL[2]	Hg (^{203}Hg)	0.092	0.6
Sb (^{124}Sb)	0.030	NL[2]	Th (^{233}Pa)	0.045	0.2
Cs (^{134}Cs)	0.018	0.5	U (^{239}Np)	0.36	1

Table VII: 43 element table of detection limits (D.L.) in parts-per-trillion measured in this study compared to D.L.s for wafer-sized samples (1-10 grams) similar to those in Reference 1. We list Element (Isotope) used in this work. Reference 1 lists only element.

[1] Interference from the $^{28}Si(n,\alpha)^{24}Na$ reaction limits the D.L..
[2] NL means the element was detected and measured and no detection limit was given. ND means not detected.

TABLE VIII

Estimated Interference-Free Detection Limits (IFDL) for 0.365 kg-sized Samples and 124 Hour Irradiations at 6.43E12 neutrons/cm^2/sec. Flux

Element	D.L. (Ref. 2)	Est. IFDL from this study
Sc (^{46}Sc)	0.002	0.00002
Cr (^{51}Cr)	0.3	0.002
Fe (^{59}Fe)	10.0	0.1
Co (^{60}Co)	0.02	0.0004
Zn (^{65}Zn)	0.7	0.005
Sb (^{124}Sb)	0.1	0.0003
Cs (^{134}Cs)	0.02	0.0003
Eu (^{152}Eu)	0.01	0.0002
Hf (^{181}Hf)	0.05	0.0003
Ta (^{182}Ta)	0.01	0.0003
Au (^{198}Au)	0.0005	0.000002
Th (^{233}Pa)	0.02	0.0002

Table VIII: Estimated Interference-Free Detection Limits (IFDL) for large (0.365 kg) samples.

References:

1) M.L. Verheijke, H.J.J. Jaspers, J.M.G. Hanssen, and M.J.J. Theunissen: Journal of Radioanalytical and Nuclear Chemistry, Articles, Vol. 113 (1987) 397-403

2) A. Huber, G. Böhm, and S. Pahlke: Journal of Radioanalytical and Nuclear Chemistry, Articles, Vol. 169 (1993) 93-104

3) M.L. Böttger, S. Niese, D. Birnstein, and W. Helbig: Activation Analysis: Journal of Radioanalytical and Nuclear Chemistry, Articles, Vol. 130 (1989) 417-423

4) F. Asaro (1994) private communication of latest values, and I. Perlman and F. Asaro: Archaeometry, Vol. 11 Cambridge University Press, Cambridge, 1969.

5) A.R. Smith and H.A. Wollenberg: Proceedings of the 2nd International Symposium on the Natural Radiation Environment, Conf-720805-P1, Aug. 7-11, 1972, p. 181-231, Houston Tx.

6) K. Debertin and R.G. Helmer: Gamma- and X-Ray Spectrometry with Semiconductor Detectors. Elsevier Science Publishing Company, Inc. New York (1988) ISBN: 0 444 871071

7) J.T. Routti and S.G. Prussin: Nucl. Instrum. & Methods 72 (1969) 125

8) C. M. Lederer and V. Shirley, Ed.: Table of Isotopes, Seventh Edition, John Wiley & Sons, Inc., New York. (1978) ISBN: 0-471-04179-3

9) E. Browne and R. B. Firestone, V. Shirley, Ed.: Table of Radioactive Isotopes, John Wiley & Sons, Inc., New York. (1986) ISBN: 0-471-84909-X

10) S. F. Mughabghab, M. Divadeenam, and N.E. Holden: Neutron Cross Sections, Academic Press, New York (1981) ISBN 0-12-509701-8

Figure Captions

Figure 1 a) Spectrum of 0.020 grams of the "standard pottery" taken 12 days after a 20 minute irradiation. Channel 6000 corresponds to 2665 keV. (Note that the full scale for the spectrum shown in Figure 1b is slightly different.)

b) Spectrum of a 6.9 gram sample of float-zone silicon taken 58 days after a 10 hour irradiation and normalized to (a). The normalization accounts for differences in neutron flux integral, mass, and counting time. Channel 6000 corresponds to 2890 keV.

Figure 2 a) Spectrum of 3.005 gram sample of float-zone silicon before etching. Full scale, channel 12000, corresponds to 2666 keV for both (a) and (b).

b) Spectrum of 3.005 gram sample of float-zone silicon after etching. These spectra are not normalized because they are taken at different times and therefore have different ratios of short- and long-lived activities.

Figure 3 Bar graph showing detection limits for 43 elements.

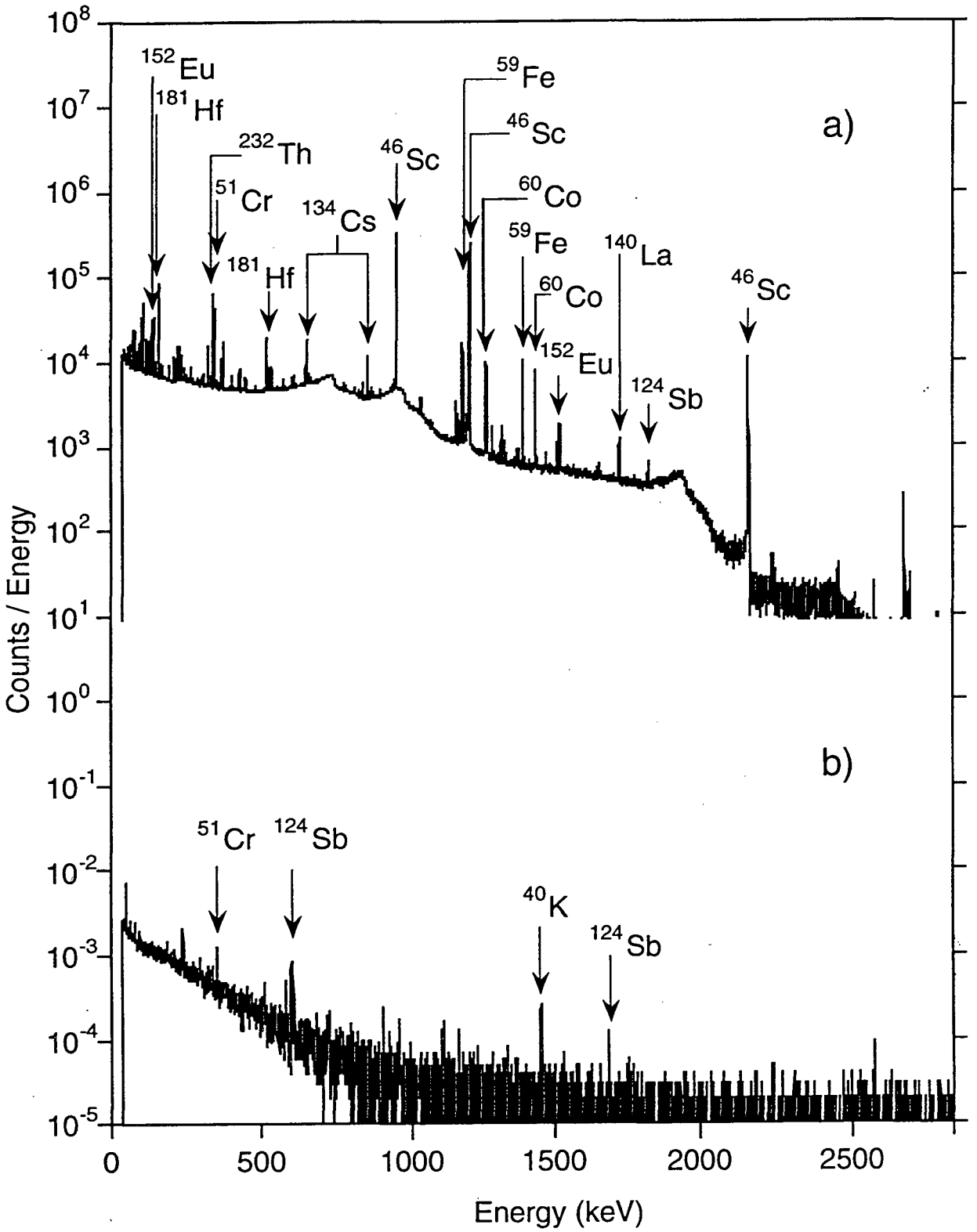

Figure 1

XBD 9505-02059.MDP

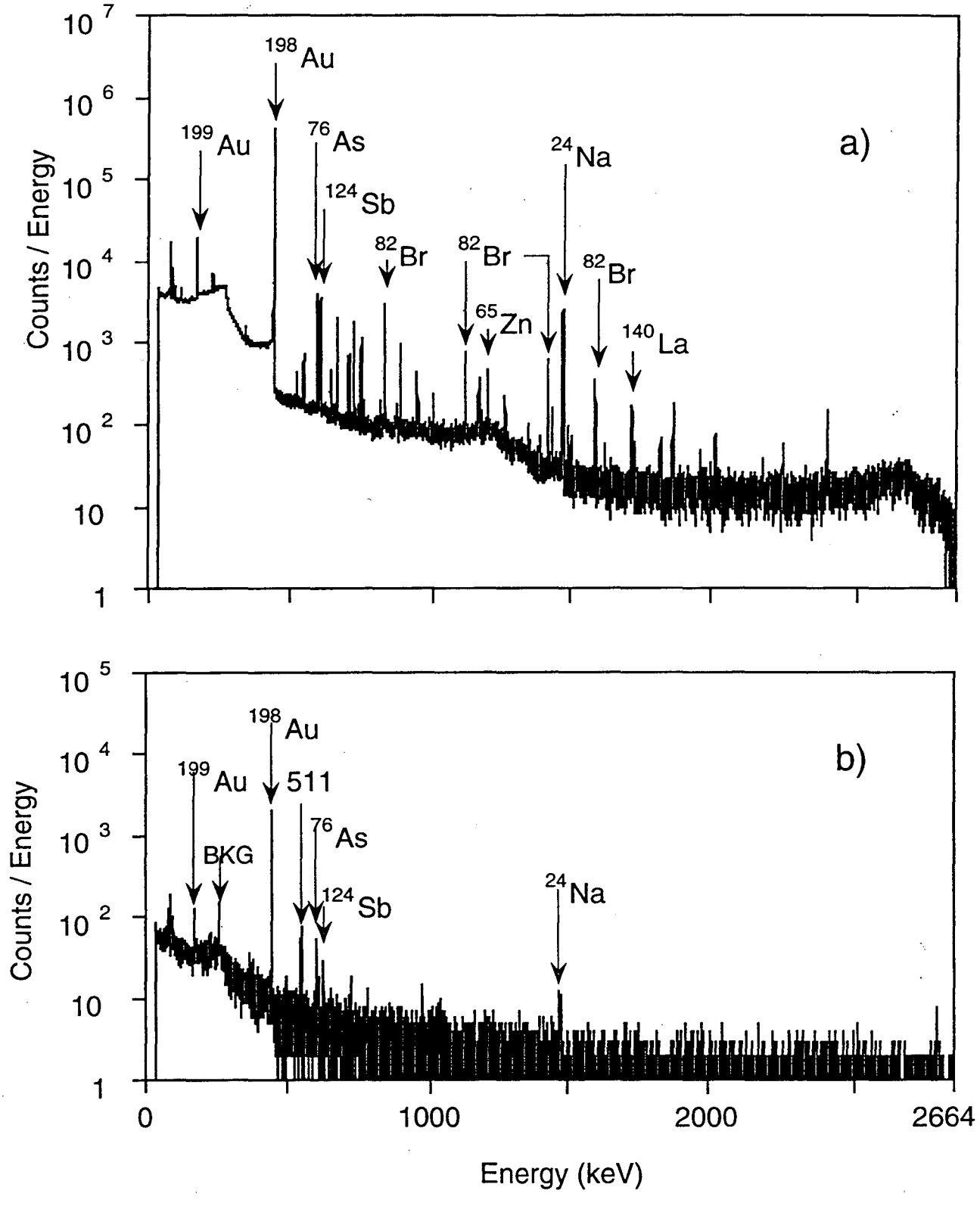

Figure 2

XBD 9505-02060.MDP

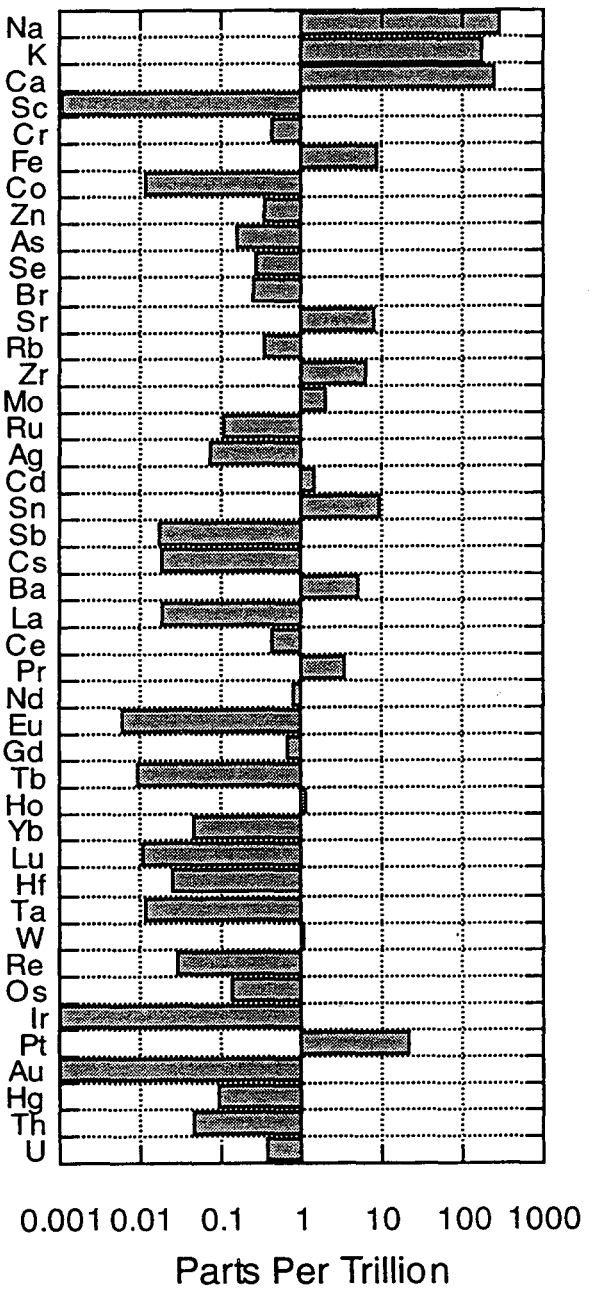

Figure 3

XBD 9505-02061 MDP

Appendix

Calculations of Concentrations:

The program PANORAMA combines aspects of a spreadsheet as well as aspects of a database. Each row contains information on a characteristic gamma ray, including peak area, detector efficiency, neutron absorption cross-section, half-life, isotopic abundance, and the relative uncertainties in these quantities. This information is then combined with run-specific information (reactor flux, counting time, sample mass, and decay time) in a MACRO calculation to compute the concentration of the element in parts-per-trillion (PPT) and the net uncertainty.

First a time correction TCorr is calculated to correct for the decay since the end of irradiation and the decay during counting:

$$\mathrm{TCorr} = \frac{\ln 2 \times \mathrm{Tc}}{\mathrm{Thalf} \times (1 - e^{-\ln 2 \times \mathrm{Tc} / \mathrm{Thalf}})} \times \frac{1}{e^{-\ln 2 \times \mathrm{TD} / \mathrm{Thalf}}} \qquad (1)$$

where the first term depends of the counting time T_C and corrects for the decay during counting and the second term depends on the delay time (T_D) between the end of irradiation and the beginning of counting. Thalf is the half-life of the isotope of interest.

The Activity (disintegrations/second) is then calculated from:

$$\mathrm{Activity} = \frac{\mathrm{PeakArea} \times \mathrm{C_I} \times \mathrm{Geo} \times \mathrm{TCorr}}{\mathrm{Eff} \times \mathrm{Tc} \times \mathrm{BR}} \qquad (2)$$

where PeakArea is the area of the characteristic gamma-ray peak, C_I and Geo are correction factors for summing and geometry, respectively (typically of the order 1 ± 0.3), TCorr is the time

correction factor defined above, Eff is the absolute detection efficiency obtained from a 5 cm diameter thin source containing 0.0404g of uranium, T_C is the counting time, and BR is the branching ratio for the gamma ray of interest.

The number of radioactive atoms calculated from the Activity in a characteristic gamma-ray peak is:

$$\text{Atoms} = \frac{\text{Activity}}{(1.0\text{E}-24) \times \text{NF} \times \text{Abu} \times (\sigma_T + f \times \sigma_R) \times (1 - e^{-\ln 2 \times T_{IRR} / \text{Thalf}})} \qquad (3)$$

where NF is the neutron flux (in units of neutrons / cm^2/sec), Abu is the abundance of the isotope being activated, σ_T and σ_R are the thermal and resonant neutron cross-sections in barns and f is the ratio of the resonant to thermal fluxes in the reactor (1.8% for our runs), T_{IRR} is the irradiation time, and the factor 1.0E-24 converts barns to cm^2.

The concentrations in parts-per-trillion are then calculated by:

$$\text{PPT} = \frac{1.0\text{E}12 \times \text{Atoms} \times \text{M}}{6.02\text{E}23 \times \text{mass}} \qquad (4)$$

where M is the atomic mass of the isotope being activated, mass is the mass of the sample being counted, 6.02E23 is Avogadro's number, and 1.0E12 converts the ratio into parts-per-trillion.

The uncertainty UPPT is calculated quadratically from the uncertainties (expressed in % for convenience and consistency) in all these quantities. The uncertainty in the half-life includes the magnifying effect of measurement following decays of several to many half-lives. The % uncertainty UT after decay time T_D is calculated from:

$$UT = \frac{UThalf \times 100}{Thalf} \times \frac{\ln 2 \times T_D}{Thalf} \qquad (5)$$

where Thalf is the half-life and UThalf is the uncertainty in the half-life.

LAWRENCE BERKELEY LABORATORY
UNIVERSITY OF CALIFORNIA
TECHNICAL AND ELECTRONIC
INFORMATION DEPARTMENT
BERKELEY, CALIFORNIA 94720